Supporting Information for

A branch-migration based fluorescent probe for straightforward, sensitive and specific discrimination of DNA mutations

*Xianjin Xiao[1,2], Tongbo Wu[1], Lei Xu[1], Wei Chen[1], Meiping Zhao[1]**

[1]Beijing National Laboratory for Molecular Sciences and MOE Key Laboratory of Bioorganic Chemistry and Molecular Engineering, College of Chemistry and Molecular Engineering, Peking University, Beijing 100871 (China)

[2]Family Planning Research Institute/Center of Reproductive Medicine, Tongji Medical College, Huazhong University of Science andTechnology, Wuhan 430030 (China)

** To whom correspondence should be addressed. Tel: 86-010-62758153; Fax: 86-10-62751708; Email: mpzhao@pku.edu.cn*

Table S1. DNA sequences used in this work.

Strand name	Sequence (from 5' to 3')[a]
BM-1 probe	3'-CATAGTATCGTATTC**GCAGTGATGA**-FAM-5' 5'-GTATCATAGCATAAG**CGTCACTACT**(-Dabcyl)TGCAGATAGTCAGTAAC-3'
BM-1A probe	3'-CATAGTATCGTATTC**GCAGTTATGA**-FAM-5' 5'-GTATCATAGCATAAG**CGTCAATACT**(-Dabcyl)TGCAGATAGTCAGTAAC-3'
BM-1T probe	3'-CATAGTATCGTATTC**GCAGTAATGA**-FAM-5' 5'-GTATCATAGCATAAG**CGTCATTACT**(-Dabcyl)TGCAGATAGTCAGTAAC-3'
PM-1 target	GTT ACT GAC TAT CTG CAA GTA GTG ACG
PM-1L target	GTT ACT GAC TAT CTG CAA GTA GTG ACG ACT GAA TGA TAT ACA
1-MM-1 target	GTT ACT GAC TAT CTG CAA GTA CTG ACG
1-MM-1A target	GTT ACT GAC TAT CTG CAA GTA ATG ACG
1-MM-1T target	GTT ACT GAC TAT CTG CAA GTA TTG ACG
1-MM-1L target	GTT ACT GAC TAT CTG CAA GTA CTG ACG ACT GAA TGA TAT ACA
1-MM-1L-T target	GTT ACT GAC TAT CTG CAA GTA TTG ACG ACT GAA TGA TAT ACA
BM-2 probe	5'-CATAGTATCGTATTC**TGGGCGGGCC**-FAM-3' 3'-GTATCATAGCATAAG**ACCCGCCCGG**T(-Dabcyl)TTGACGACCCACGC-5'
PM-2 target	TGG GCG GGCC AAA CTG CTG GGT GCG
1-MM-2 target	TGG GCT GGCC AAA CTG CTG GGT GCG
BM-3 probe	3'-CATAGTATCGTATTC**GTTGTGGGAA**-FAM-5' 5'-GTATCATAGCATAAG**CAACACCCTT**-(Dabcyl)CCACTGTACTTCATACATG
EGFR wild-type template	TCT GAC CTA CAAATA TTT ACA GAA ACC CAT GTA TGA AGT ACA GTG GAA GGT TGT TGA GGA GAT AAA TGG AAA CA
EGFR mutant-type template	TCT GAC CTA CAAATA TTT ACA GAA ACC CAT GTA TGA AGT ACA GTG GAA GGT TGT TGA GGG GAT AAA TGG AAA CA
Phosphate forward primer	5'-PO_4-TGT TTC CAT TTA TCT CCT CAA-3'
Reverse primer	TCT GAC CTA CAA ATA TTT ACA GA
BM-4 probe	3'-GTTATGCTATGATACG**TAAAGAGACA**-FAM-5' 5'-CAATACGATACTATGC**ATTTCTCTGT**-(Dabcyl)AGCTAGACCAAAATCACC-3'
BRAF Wild-type template	ACC TCA CAG TAA AAA TAG GTG ATT TTG GTC TAG CTA CAG TGA AAT CTC GAT GGA GTG G
BRAF mutant-type template	ACC TCA CAG TAA AAA TAG GTG ATT TTG GTC TAG CTA CAG AGA AAT CTC GAT GGA GTG G
Forward primer BRAF	CCACAGAGACCTCAAGAGTAAT
Reverse primer BRAF	5'-PO_4-GGACCCACTCCATCGAGATTT

[a] The sequences of the branch migration region are shown in bold.

Table S2. Increase rates of fluorescence intensity of different BM probes in the absence[a] and presence[b] of Vent exo$^-$ polymerase.

Experiment	Base pairs	Increase rate of fluorescence intensity (a.u./s)
BM-1 probe + PM-1 target	C:G	1.53±0.08
BM-1 probe + 1-MM-1 target	C:C	0.0738±0.0008
BM-1 probe + PM-1 target + vent exo$^-$	C:G	2.30±0.18
BM-1 probe + 1-MM-1 target + vent exo$^-$	C:C	0.00742±0.00052
BM-1 probe+1-MM-1T target + vent exo$^-$	C:T	0.00983±0.00071
BM-1 probe+1-MM-1A target + vent exo$^-$	C:A	0.0124±0.0010
BM-1A probe + 1-MM-1T target + vent exo$^-$	A:T	2.43±0.17
BM-1A probe + PM-1 target + vent exo$^-$	A:G	0.246±0.018
BM-1A probe + 1-MM-1 target + vent exo$^-$	A:C	0.0192±0.0005
BM-1A probe + 1-MM-1A target + vent exo$^-$	A:A	0.0272±0.0008
BM-1T probe + 1-MM-1T target + vent exo$^-$	T:A	2.20±0.16
BM-1T probe + PM-1 target + vent exo$^-$	T:G	0.129±0.009
BM-1T probe + 1-MM-1 target + vent exo$^-$	T:C	0.0163±0.0012
BM-1T probe + 1-MM-1T target + vent exo$^-$	T:T	0.0488±0.0030

[a]BM probe concentration: 200 nM; Gain level: 7.33.

[b]BM probe concentration: 100 nM; Gain level: 9.

Theoretical calculation of the ratio of the discrimination factors (DF) toward perfect-match target and single-base mismatched target between the branch migration process and the toehold exchange process

The kinetic modeling of strand displacement established by Erik Winfree (S1) is illustrated in the figure below:

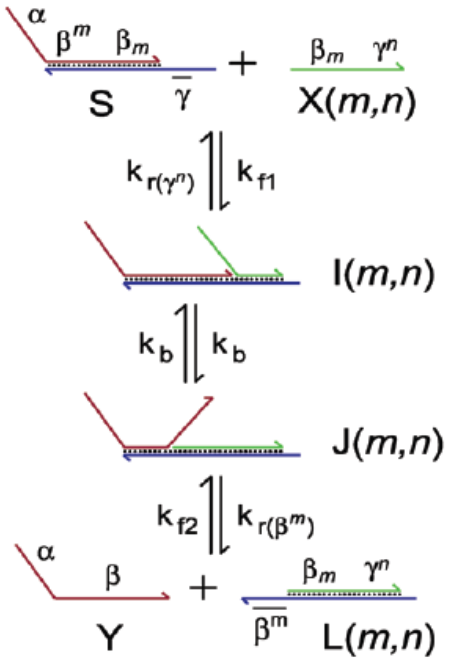

The associated forward second-order rate constant for this bimolecular reaction model of strand displacement is as follows:

$$k_{(\beta^m,\beta_m,\gamma^n)} \equiv \frac{k_{r(\beta^m)} k_f k_b}{k_{r(\gamma^n)} k_{r(\beta^m)} + k_{r(\gamma^n)} k_b + k_{r(\beta^m)} k_b}$$

Where $k_f = 3.5 * 10^6 M^{-1} s^{-1}$ (usually)

$k_b = \frac{400}{x^2} s^{-1}$, where x is the length of the branch migration domain.

$k_{\gamma(\delta)} = k_f * \frac{2}{x} * e^{\Delta G^{\emptyset}(\delta)/RT} s^{-1}$, where $\Delta G^{\emptyset}(\delta)$ is the standard free energy of binding of toehold δ

Herein, the length of the γ^n domain is similar to that of the β^m domain. Therefore, the above expression can be simplified as:

$$k_{(toehold\ exchange\ probe)} = \frac{k_f k_b}{k_{r(\gamma^n)} + 2k_b}$$

When there exists a mismatch between the invading strand and the incumbent strand within the branch migration domain, the above equation would change to:

$$k_{(toehold\ exchange\ probe,mismatch)} = \frac{k_f k_{b'}}{k_{r(\gamma^n)} + k_b + k_{b'}}$$

Where $k_{b'}$ is the rate constant of mismatched branch migration process.

Therefore,

$$\frac{k_{(toehold\ exchange\ probe)}}{k_{(toehold\ exchange\ probe,mismatch)}} = \frac{k_b}{k_{b'}} \times \frac{k_{r(\gamma^n)} + k_b + k_{b'}}{k_{r(\gamma^n)} + 2k_b}$$

For BM probe, the binding process is illustrated as follows:

$$X + S \underset{k_{r(\gamma^n)}}{\overset{k_f}{\rightleftharpoons}} I \underset{k_b}{\overset{k_b}{\rightleftharpoons}} J$$

The length of the toe is 17 nt, and the corresponding $\Delta G^{\emptyset}(\gamma^n)$ is around 120 kJ/mol. Therefore,

$$k_r = k_f * \frac{2}{x} * e^{\Delta G^{\emptyset}/RT} s^{-1} \approx 0$$

Also, $k_f \gg k_b$. Therefore, the reaction rate is controlled by the second step,

$$k_{(BM\ probe)} = \frac{d[J]}{dt} = k_b[I] - k_b[J]$$

At the early stage of the whole reaction, we could neglect the reverse reaction of J to I. Then,

$$k_{(BM\ probe)} = k_b[I]$$

Following the above procedure, we could obtain the expression for $k_{(BM\ probe)}$:

$$k_{(BM\ probe,mismatch)} = k_{b'}[I]$$

$$\frac{k_{(BM\ probe)}}{k_{(BM\ probe,mismatch)}} = \frac{k_b}{k_{b'}}$$

Then,

$$\frac{DF(toehold\ exchange\ probe)}{DF(BM\ probe)} = \frac{k_{r(\gamma^n)} + k_b + k_{b'}}{k_{r(\gamma^n)} + 2k_b}$$

Where,

$$k_b = \frac{400}{x^2} s^{-1} = \frac{400}{10^2} = 4s^{-1}$$

$$k_{\gamma(\delta)} = k_f * \frac{2}{x} * e^{\frac{\Delta G^{\emptyset}(\delta)}{RT}} s^{-1} = 3.5 \times 10^6 \times \frac{2}{10} \times e^{\frac{-40000}{8.314 \times 298}} = 0.068 s^{-1}$$

Also,

$$k_{b'} \ll k_b$$

Therefore,

$$\frac{DF(toehold\ exchange\ probe)}{DF(BM\ probe)} = \frac{k_{r(\gamma^n)} + k_b + k_{b'}}{k_{r(\gamma^n)} + 2k_b} \approx \frac{k_b}{2k_b} = \frac{1}{2}$$

It's worth to note that above model can only accurately predict the kinetics of strand displacement processes when the concentrations of invading strand and substrate complex are sufficiently low (about nM level) (S1). At higher concentrations of invading strand (>300 nM) and substrate complex (>100 nM), the experimentally observed reaction kinetics were significantly slower than those predicted by the model. This may partially explain why the experimentally observed DFs were usually lower than the theoretical predicted DFs.

Optimization of the length of the branch migration region

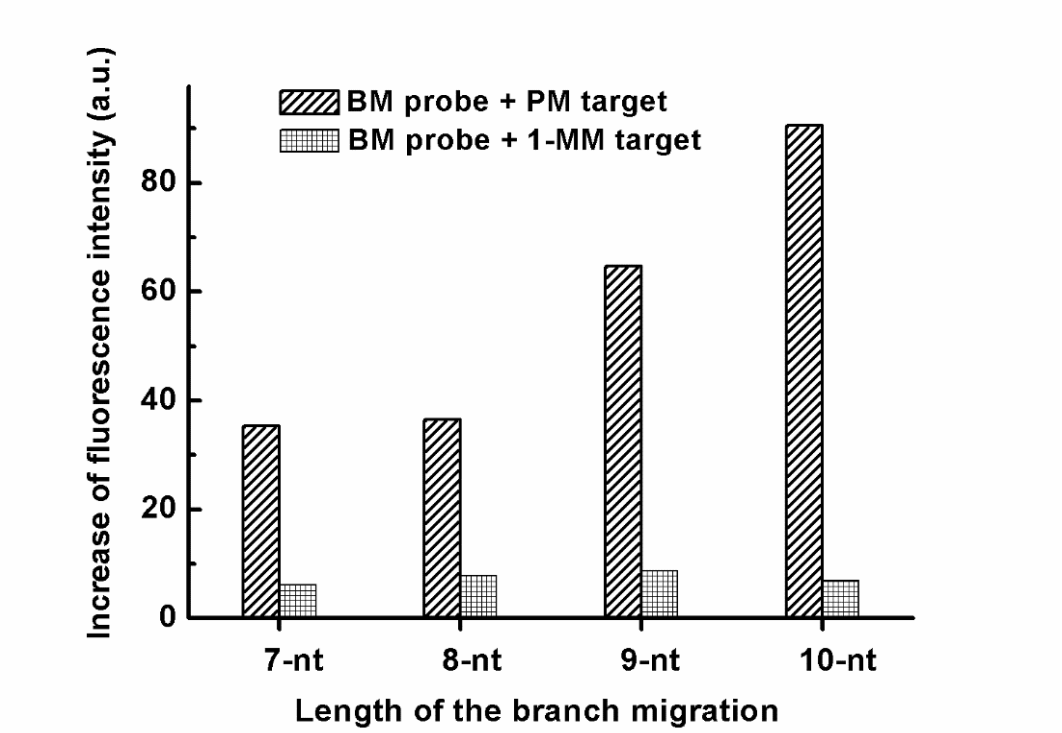

Figure S1. The signal of MB-1 probe toward PM-1 target and 1-MM-1 target with the length of the branch migration varied from 7-nt to 10-nt. The increase of fluorescence intensity was calculated as the difference between the initial fluorescence intensity and the plateau fluorescence intensity.

Optimization of the position of the fluorophore

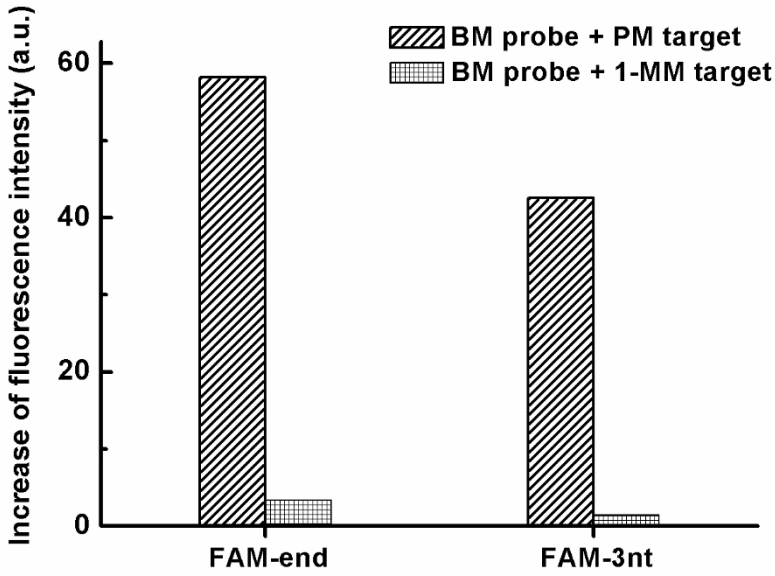

Figure S2. The signal of MB-1 probe toward PM-1 target and 1-MM-1 target with the position of the fluorophore changing from the 5' end to the location 3-nt away from the 5' end.

Discrimination of C:C mismatch at different positions

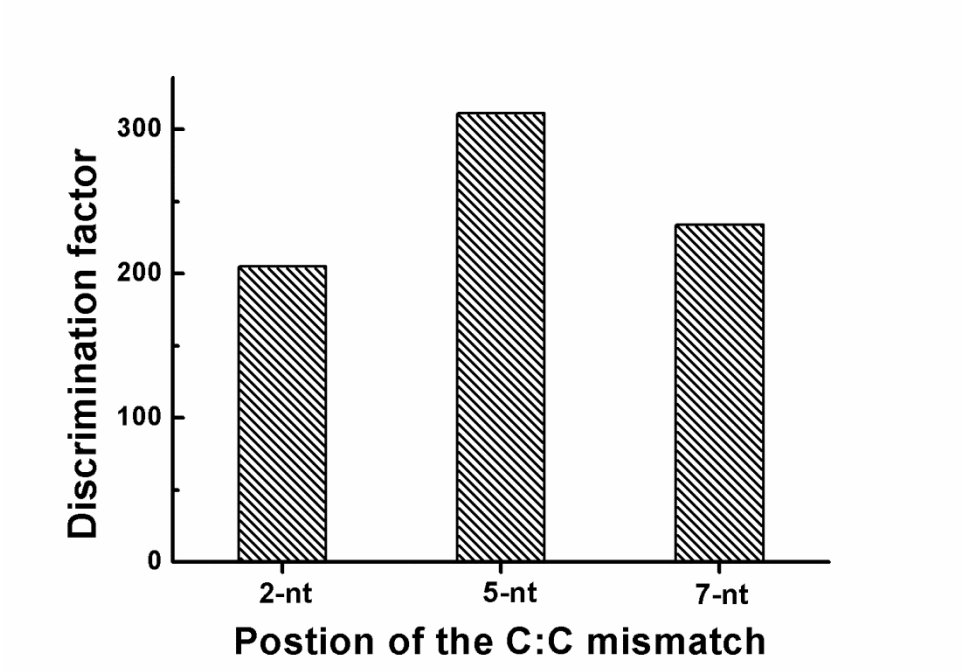

Figure S3. Discrimination of C:C mismatch at different positions. We tested three positions: 2-nt, 5-nt and 7-nt away from the 5' end of the S-strand.

Detection of low-abundance PM-1 target at 33 °C (C:C mismatch)

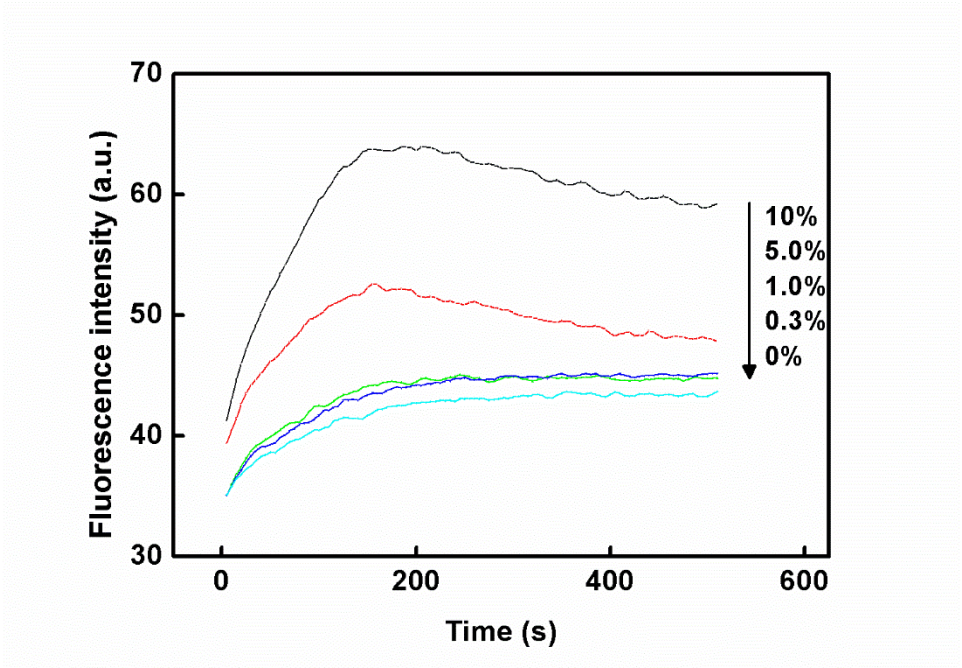

Figure S4. The fluorescence intensity responses of BM probe toward PM targets with different abundances at 33 °C

Detection of low-abundance PM-1 target at 28 °C (C:C mismatch)

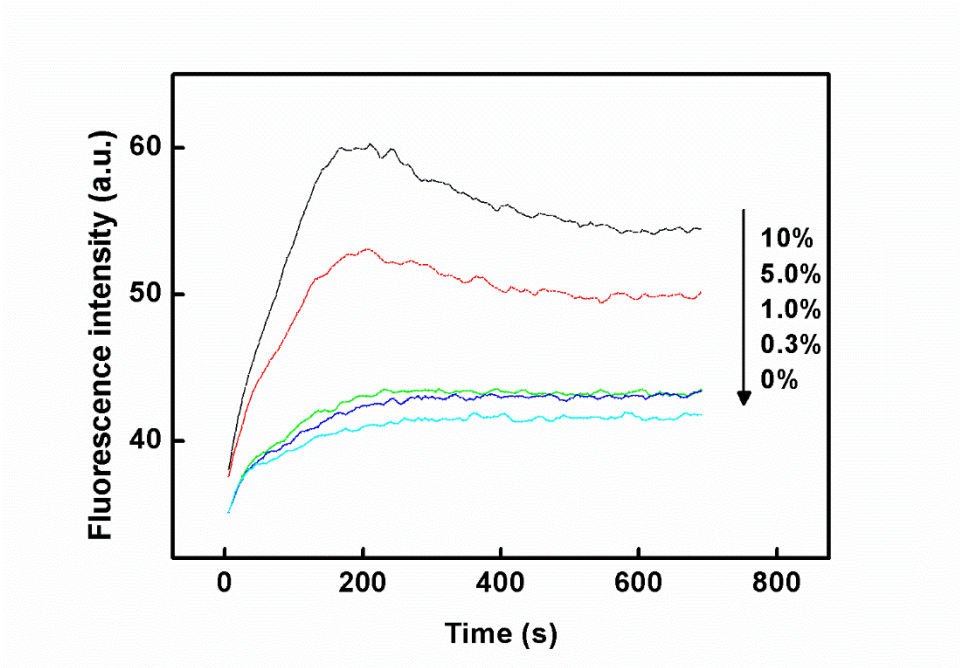

Figure S5. The fluorescence intensity responses of BM probe toward PM targets with different abundances at 28 °C

Detection of low-abundance PM-1 target at 25 °C (C:C mismatch)

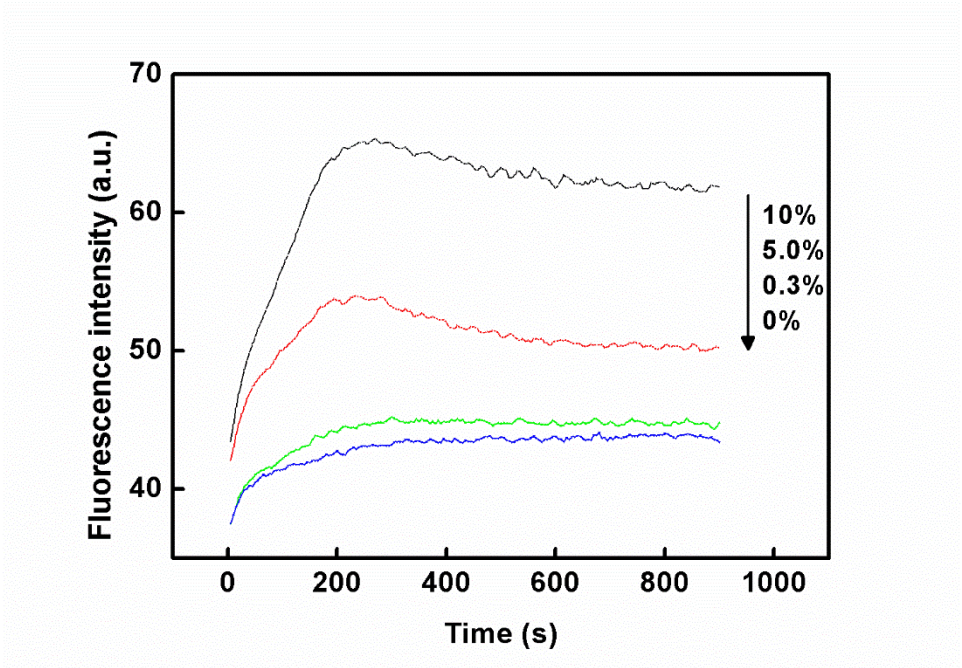

Figure S6. The fluorescence intensity responses of BM probe toward PM targets with different abundances at 25 °C

Detection of low-abundance 1-MM-1T target by BM-1A probe (A:A mismatch).

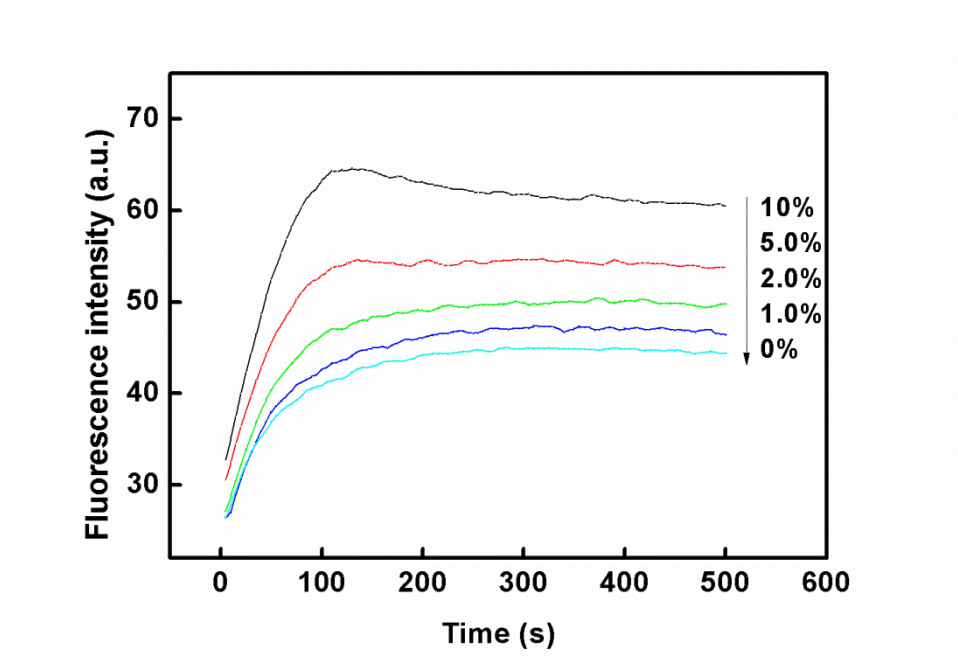

Figure S7. The fluorescence intensity responses of BM-1A probe toward 1-MM-1T targets with different abundances. The interfering sequences were 1-MM-1A targets (A:A mismatch).

Sanger sequencing of the PCR products of the cfDNA extracted from the serum of a thyroid cancer patient.

Figure S8.Sequencing result of the PCR products of the cfDNA extracted from the serum of a thyroid cancer patient. The abundance of BRAF V600E mutation in the tested patient was lower than the detection limit of Sanger Sequencing, as indicated by the arrowed peak.

REFERENCES

S1. Zhang, D.Y. and Winfree, E. (2009) Control of DNA Strand Displacement Kinetics Using Toehold Exchange. *J. Am. Chem. Soc.*, **131**, 17303-17314.